Hybrid strontium bromide-natural graphite composites for low to medium temperature thermochemical energy storage:

Cammarata, A.; Verda, V.; Sciacovelli, Adriano; Ding, Yulong

DOI:
10.1016/j.enconman.2018.04.031

Document Version
Peer reviewed version

Citation for published version (Harvard):
Cammarata, A, Verda, V, Sciacovelli, A & Ding, Y 2018, 'Hybrid strontium bromide-natural graphite composites for low to medium temperature thermochemical energy storage: Formulation, fabrication and performance investigation', *Energy Conversion and Management*, vol. 166, pp. 233-240.
https://doi.org/10.1016/j.enconman.2018.04.031

Hybrid Strontium Bromide-Natural graphite composites for low to medium temperature thermochemical energy storage: Formulation, fabrication and performance investigation

A Cammarata[a], V Verda[a], A. Sciacovelli[b*], Y. Ding[b]

[a]Department of Energy, Politecnico di Torino, Turin, 10129, Italy
[a]Birmingham Centre for Energy Storage, School of Chemical Engineering, University of Birmingham, Birmingham, B15 2TT, UK
* Corresponding author. Email: a.sciacovelli@bham.ac.uk; Tel. +44 (0)121 414 8747;

Abstract

Thermochemical energy storage has the potential to provide efficient, compact and long duration storage of thermal energy. Major advancements, however, are needed for such a technology to meet performance and cost targets. Here we present a study on novel composites for low to medium temperature thermochemical energy storage (<150°C) with an aim to maximize energy density and to understand the associated mass and heat transport phenomena. The composites were made of strontium bromide hexahydrate and natural graphite with the latter acting as a supporting matrix. We used a simple manufacturing method to fabricate the composites and experimentally characterized the performance of the materials using various methods including thermogravimetry, laser flash analysis and dynamic vapor sorption. The results showed that the composites achieved an energy density above 600kJ/kg with the storage process occurring mostly below ~100°C – a promising feature for domestic applications. The results also showed that the natural graphite could improve the hydration-dehydration kinetics by reducing hysteresis and a four-fold increase in the thermal conductivity could be achieved with 20% of natural graphite in the composite.

Introduction

Recent years have seen increased demands for effective and efficient thermal energy storage (TES) technologies for clean heat and cold supply, which currently accounts for 40-60% of final energy consumption in most of the counties [1–3]. This is driven by the needs for increasing renewable energy penetration and decarbonisation of heating & cooling, as well as harnessing waste heat/cold and peak shaving of energy networks. There are three types of TES technologies based respectively on sensible heat, latent heat and reversible thermochemical processes. Thermochemical based method has the potential to store 8-20 times more thermal energy per unit of mass of storage material than the sensible and latent heat based TES technologies, and has therefore attracted significant attention in the past decade [4–8]. However, the technology readiness level of the thermochemical storage (TCS) is still low and has multiple challenges including life span and stability of storage materials, efficient thermochemical reactors and integration and TCS system costs. These challenges have been hindering the industrial uptake of technology [9–12].

The work presented in this paper concerns TCS for domestic applications with a focus on operations at a low to medium temperature range (50°C-150°C) due to safety considerations. Over the temperature range, salt hydrates are regarded as the most promising TCS materials for which numerous material systems have been proposed in the literature [13–15]. Most of them, however, are unable to meet the criteria for use in a domestic environment. N'Tsoukpoe et al. carried out screening of 125 salts and showed that the most promising salts were $SrBr_2 \cdot 6H_2O$, $LaCl_3 \cdot 7H_2O$ and $MgSO_4 \cdot 6H_2O$ [13]. Fopah-Lele and Tamba suggested that $SrBr_2$ $6H_2O$ was the best candidate when an external free source of heat was available for the evaporation of water [16]. As a result, the hybrid strontium bromide was targeted in this work. Figure 1 shows a schematic diagram using a domestic building as an example where solar thermal energy from vacuum solar panels (up to ~150°C) and/or other renewable heat produced by a heat pump driven by electricity from wind and solar energy is stored in the TCS system.

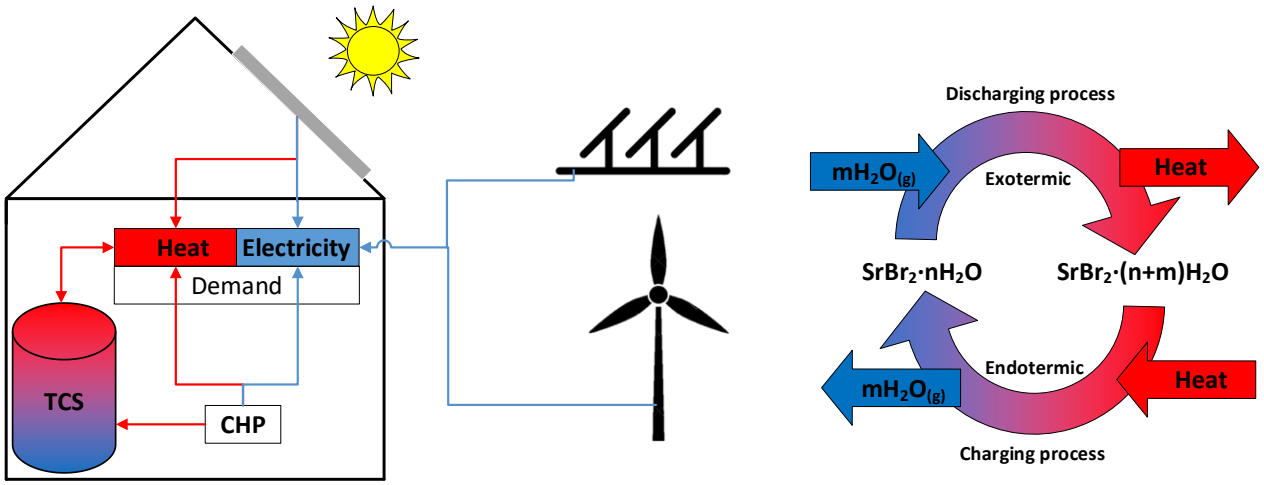

Fig. 1. A thermochemical storage (TCS) device for a household application (Left); a schematic of thermochemical reaction (hydration/dehydration) for thermal energy storage (Right).

The TCS shown in the figure is based on the reversible hydration/dehydration reaction of the targeted hydrate as discussed above. During the charge process, heat is supplied to break the chemical bods between the salt (also termed sorbent) and water molecules (also called sorbate), resulting in the release of water in the form of H_2O vapor. The sorbate is either condensed for use in the discharge process, in the case of a closed TCS system, or released into the environment in the case of an open TCS system. The discharging process occurs through an exothermic hydration reaction when water vapor combined with the salt, releasing the stored heat. Equation (1) illustrates the reversible reaction.

$$SrBr_2 \cdot 6H_2O \rightleftharpoons SrBr_2 + 6H_2O_{(g)} + \Delta H_r \quad (1)$$

The use of pure salt hydrates as TCS materials come across a number of challenges including heat and mass transfer limitations induced mainly by structural change and shape stability of TCS materials. This is similar to the challenges in the use of pure phase materials in the latent heat storage and also chemical looping technology. The use of composite TCS materials have the potential to overcome the challenges and, as a result, a number of studies have been carried out in recent years. These studies used various salts (e.g. $MgSO_4$, $CaCl_2$ and LiBr) in different structural materials including zeolite, silica gel and activated carbon [12,17,18]. Composite TCS containing $SrBr_2$, however, remains largely unexplored, and the published studies were primarily on energy storage density [19–21] or on the performance of pure $SrBr_2$ at the reactor scale [8,22] [23]. To our knowledge, no studies have been published on linkage between the performance and structure of the composite TCS containing $SrBr_2$ – the main motivation of this paper. In this work, we used natural graphite as the structural material (matrix host) for the $SrBr_2$ based TCS composites. A simple manufacturing processes is proposed and used to fabricate the composite. We found, for the first time, how the composite formulation affect the energy density, heat and mass transfer, and reaction kinetics. Our work investigates for the first time the links between formulation and thermal properties of TCS composites, including enhancement in thermal conductivity and specific heat, which are shown to impact significantly on total energy density.

Manufacturing and characterisation of TCS composites

Manufacturing Process

Figure 2 illustrates schematically the manufacturing process of TCS composites. Natural carbon graphite supplied by Inoxia Ltd UK with the following composition 98.6% Carbon, 0.05% Sulphur, 0.05% Nitrogen,

0.8% ash, 0.3% Volatile and 0.3% Moisture was used; from the previous composition and from the molecular weight of H_2O we estimated a 0.27% of O content in the graphite. The graphite was initially dried in oven at 150°C for 12 hours to remove any trace of moisture, as depicted in Fig 2. A water solution of strontium bromide ($SrBr_2$, chemical reagent grade, Aldrich) was then prepared using distilled water. The amounts of water and salt were set in such a way to achieve a salt content of 40% or 80% (by mass) in the final dry TCS composites. A wet impregnation process was then followed to fabricate the TCS composites, which involved the addition of the salt solution at a slow and constant rate to the graphite particle bed with the bed being stirred. The solution addition process was carefully controlled so that the particle bed appeared to be dry macroscopically with the salt solution fully drawn into the intraparticle pores of the particle bed. This resulted in a wet mass of the composite, which was then placed in an oven to remove the water in the matrix and dehydrate the salt. A minimum drying temperature of 200°C was chosen to ensure full dehydration of the salt. Finally, the dehydrated TCS material was then shaped using die-plunge device in a Lloyd LS100Plus testing machine to give circular tablets of 13 mm diameter and a thickness between 1 and 2 mm; see Fig. 3.

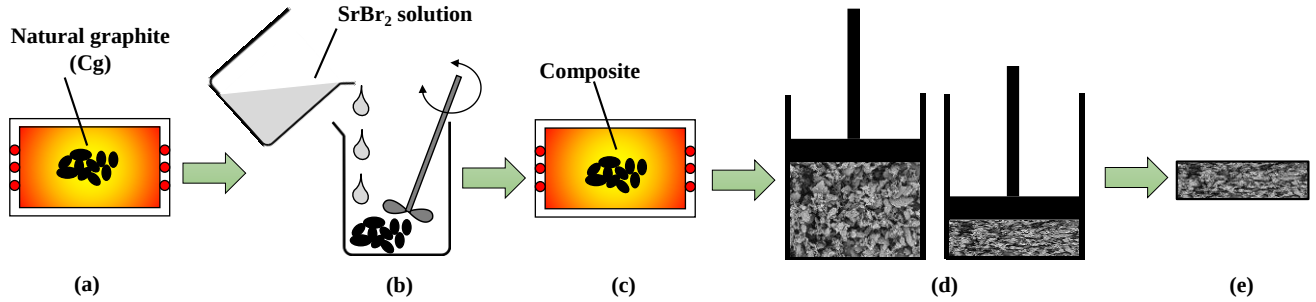

Fig. 2. Manufacturing process of TCS composites: a) drying of natural graphite; b) wet impregnation of Cg with water solution of $SrBr_2$; c) drying of the salt impregnated Cg; d) tableting of the salt impregnated Cg; e) final composite TCS tablet.

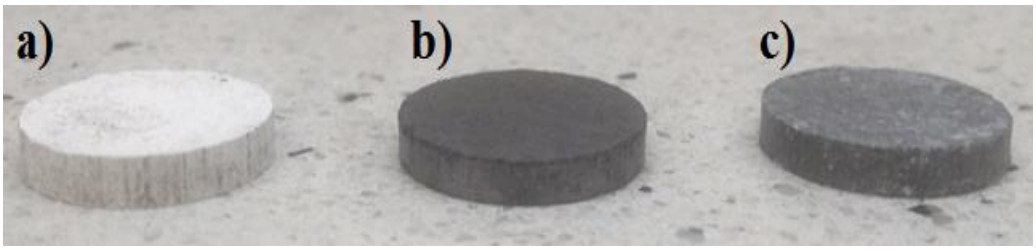

Fig. 3. Composite TCS samples: a) pure $SrBr_2$; b) TCS composite with 40% $SrBr_2$; c) TCS composite with 80% $SrBr_2$.

Characterization of TCS composites

Scanning electron microscopy (SEM): the TCS materials were imaged using a Hitachi TM3030 scanning electron microscope equipped with energy dispersive X-ray spectroscopy (EDX); A 5kV accelerating voltage was used for the observations whereas the EDX analysis was carried out at 15kV. The TCS samples were coated with a 5nm layer of gold using a Quorum Q150T sputter coater in order to avoid the charge-up phenomenon.

Specific surface characterization: Nitrogen physisorption was performed using a Micromeritics ASAP 2020 plus. For doing so, TCS composite samples of 0.4-0.5g were dried and degassed at 250°C for overnight before measurements to remove moisture and any gas adsorbed. Both adsorption and desorption isotherms were

obtained using nitrogen as gas adsorbate and an equilibrium time of 5 min was adopted at each relative pressure p/p_0. Specific surface area was then derived from the isotherms using a multipoint Brunauer–Emmett–Teller (BET) method.

Differential scanning calorimetry: The heat of reaction, and the onset and peak temperatures of the TCS composite were measured with a differential scanning calorimeter from Mettler-Toledo (DSC2+) equipped with a robotic sampling unit for automatic measurements. For such measurements, samples of ~10mg obtained from the TCS composites were first placed in closed platinum crucibles and then positioned in the robotic sampling unit of the DSC. The DSC measurements then took place by heating the sample up from 20°C to 300°C at a heating rate of 5°C/min (with a 10min isothermal holding period at the initial/final temperature) under a constant N_2 flow of 50ml/min. The specific heat of the TCS composites was obtained by comparing DSC signal (heat flux) with the DSC signal obtained for a synthetic sapphire standard under the same conditions (DIN 51007).

Thermo-gravimetric analysis (TG): The thermochemical reaction was investigated with a Netzsch TG 209 F3 thermal gravitational analyzer (TGA). In a typical, approximately 10 mg hydrated TCS composite was placed in the TGA sample holder and heated from 20°C to 300°C at a heating rate of 5°C/min under a constant flow of nitrogen (50ml/min), with the mass change, and the onset and peak temperatures recorded during the process. Prior to TG measurements the samples were hydrated in a custom-made humidity chamber coupled with weight measurements and hence a precise control of the extent of the sample hydration.

Laser flash analysis: The thermal diffusivity of the TCS composites was determined using a laser flash apparatus (LFA 447 from Netzsch). The measurements were performed on cylindrical TCS composite pellets with a diameter of 13mm and a thickness of 1-2mm over a temperature range between 50°C and 250°C with 50°C intervals. Three pellets were analyzed for each of the composite PCM to ensure statistically meaningful results. During the measurements the pellets were exposed to 0.8ms laser pulses at each temperature and the subsequent thermal response of the pellets was post processed using a Cowan method to obtain the thermal diffusivity. Given the definition of the thermal diffusivity, $\alpha = k/\rho c_p$, where k is the thermal conductivity, ρ the density and c_p the specific heat capacity, the thermal conductivity could be obtained.

Dynamic vapor sorption analysis (DVS): The hydration/dehydration of the TCS composites was characterized using a DVS-Advantage instrument supplied by Surface Measurement Systems. Samples of ~10mg were first dried *in-situ* and then exposed to a relative humidity of RH=50% for 6 hours, followed by exposure to a RH=0% humidity also for 6 hours. Both the hydration and dehydration steps were performed at 25°C. The mass variation of the samples was recorded over the entire experiment with a time step of 20 s, enabling the investigation of both the forward and reverse reactions of the TCS composites.

Results and discussion

Figure 4 shows the SEM micrographs of the carbon graphite (Cg, Fig. 4a) and the TCS composites with 40% and 80% $SrBr_2$ (Figs. 4b and 4c respectively) at a 400x magnifications. One can see how the wet impregnation process, and therefore the inclusion of SrBr2, affects the microstructure of the TCS composite. The natural carbon graphite (Fig. 4a) shows typical lamellar, plate-like structure of an order of 50 μm in diameter. The lamellar structure disappears in TCS composites, suggesting the salt entrapment within the composites. The TCS composite containing 80% $SrBr_2$ presents a round-shaped feature with a size ~100-200 μm, whereas the size of the composite containing 40% salt is far smaller <~100 μm, indicating that an increase in the amount of salt in the composite leads to an increased characteristic size of the particles.

Figure 5 shows the elemental analysis of the TCS composites. One can see clearly from the spectrum peaks that the presence of Sr and Br elements in the sample, and the intensities of Sr and Br peaks for the TCS composite sample with 80% $SrBr_2$ are nearly twice that with 40% $SrBr_2$, suggesting the reliability of the manufacture process. Traces of oxygen can also be seen likely due to tiny hydration of the TCS composite upon in contact

with ambient air during the preparation of the EDX experiments. A minimal amount of oxygen could be due to the moisture content of the graphite, although the fabrication process (Fig 2) aims at removing such traces of moisture by pre-treating the graphite. Furthermore, the EDX spectrum shows an higher oxygen peak for composite with lower graphite content (80% of $SrBr_2$, 20% of graphite); this reinforces the conclusion that O presence is ascribable to tiny hydration of TCS composite, since the potential contribution due to graphite impurity is proportional to the graphite content in the composite. Any presence of H (due to moisture content) could not be detected by cause of intrinsic limitation of EDX technique, which is not suitable for identifying very light elements [24]

Table 1

Summary of the TCS composite materials

Sample	$SrBr_2$	$SrBr_2$40%	$SrBr_2$80%
Strontium bromide content (wt %)	100%	40%	80%
BET specific area [m2/g]	-	2.05	0.85
Heat of reaction (kJ/kg)	952.7	417.0	798.0
Specific heat [kJ/(kg K)]	0.5	0.7	1.0
Thermal conductivity at 50°C [W/(m K)]	0.38	2.30	1.33

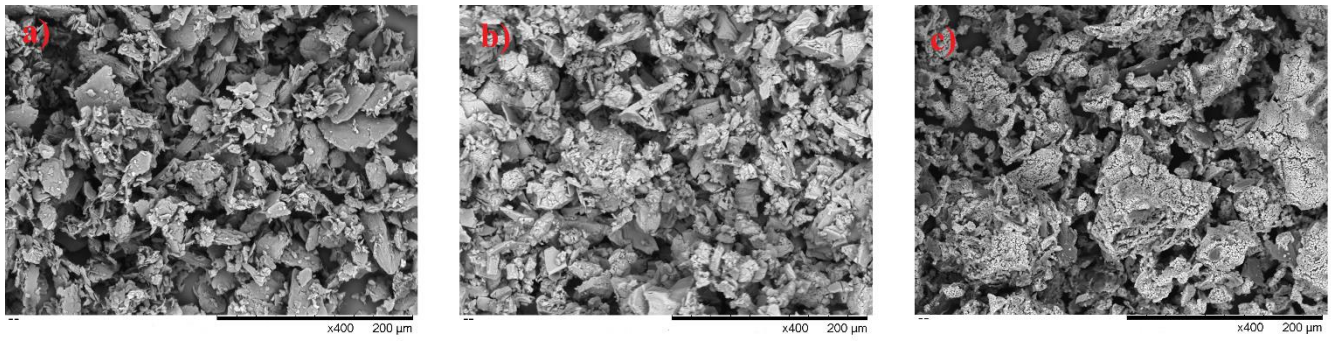

Fig. 4. Scanning electron Microscopy (SEM) of TCS composites tablets: a) Natural carbon graphite; b) TCS composite with 40% of $SrBr_2$; c) TCS composite with 80% of $SrBr_2$. The graphite shows a typical lamellar structure which are not seen from the composites containing 40% and 80% of $SrBr_2$.

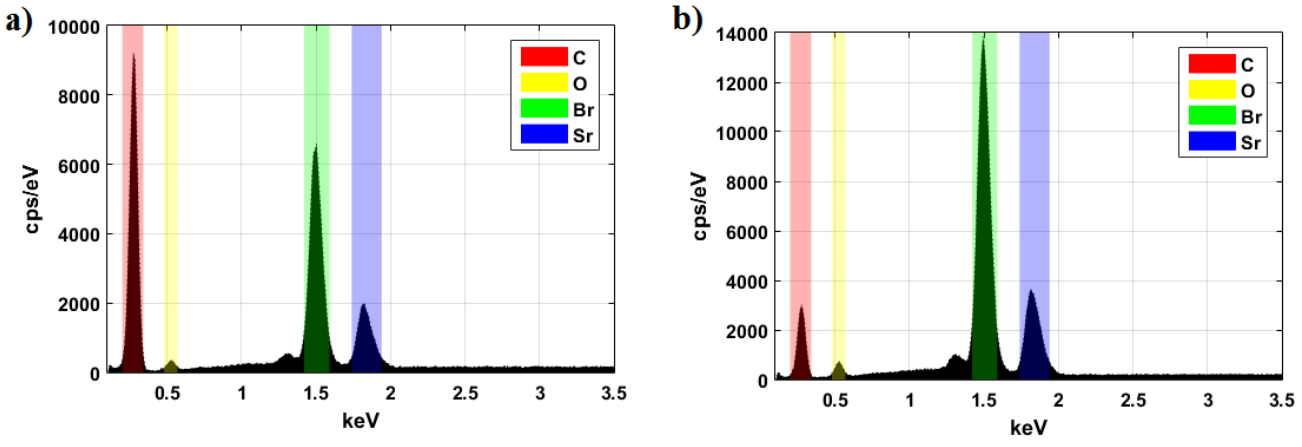

Fig. 5. Energy dispersive X-ray spectrums (EDX): a) TCS composite with 40% $SrBr_2$; b) TCS composite with 80% $SrBr_2$. Relative intensity of the peaks intensities corresponding to the amounts of strontium and of bromine

in the composites. Traces of oxygen detected due to tiny hydration of the composites during the preparation of the EDX experiments.

The results of the nitrogen physisorption analyses are shown in Figure 6 and also Table 1. The specific surface area of the TCS composites decreases significantly due to the addition of $SrBr_2$ in the formulation. This agrees well with the SEM analyses that the dimension of the microstructural features of the TCS composites increases with increasing salt concentration in the composites. The sorption data in Figure 6a exhibit isotherms of the IUPAC Types II and IV classifications [25]. The overall low adsorption capacity suggests the presence of macroscopic pores (>100 nm), which is supported by the fact that the adsorbed amount does not show a sharp increase at $p/p_0 \rightarrow 1$. The absence of an isothermal knee (the so-called Point B [25]) indicates both monolayer and multilayer adsorption phenomena. The hysteresis of the isotherms is believed to be associated with the filling and emptying of mesopores by capillary condensation [26]. The hysteresis is a typical H3-type isotherm [25] due to aggregates of platy particles. This agrees very well with SEM analyses that the natural graphite is mostly constituted of plate-like particles. This feature, however, is progressively lost with increasing content of SrB_2 in the TCS composites as evidenced by comparing the TCS composites with 40% and 80% of SrB_2 in Figure 6a. This again agrees with the SEM analyses that only rounded-like features are observed from the TCS composites with 40% and 80% of SrB_2 (Figure 4c). Finally, the sudden closure of the isotherm loops is due to sudden drop in adsorbed volume during desorption referred as the Tensile Strength Effect phenomenon [26].

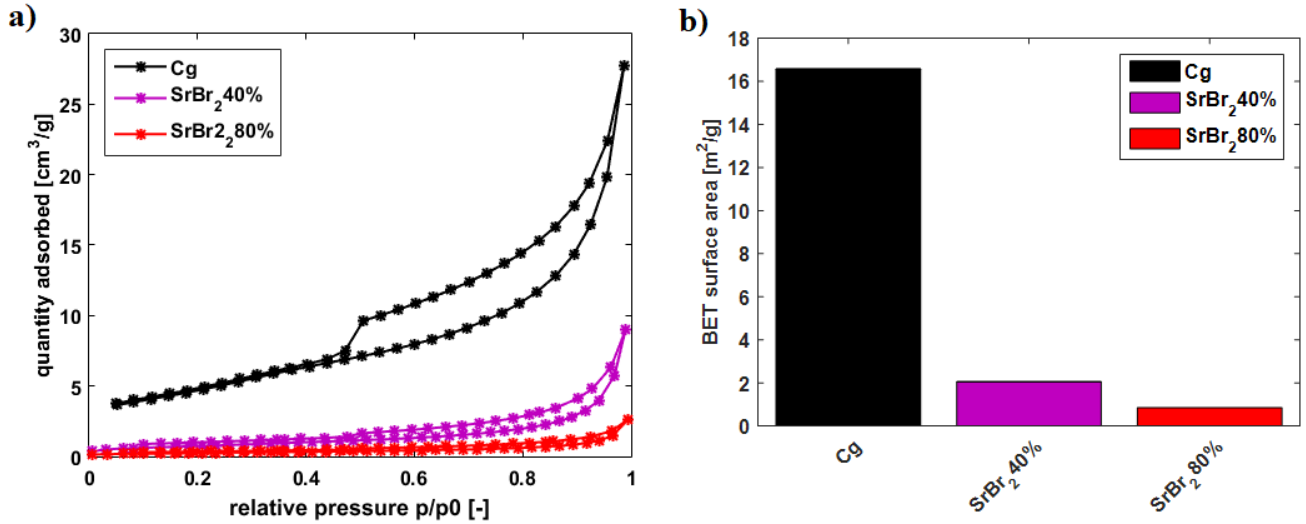

Fig. 6. a) N_2 adsorption/desorption isotherms of TCS composites with different contents of $SrBr_2$; b) Specific surface area determined by multipoint Brunauer–Emmett–Teller (BET) analysis. The isotherms show a H3 type of hysteresis loop according to the IUPAC classification; the sudden closure of the loop along the desorption branch in the p/p_0 range 0.4 – 0.5 is attributed to the Tensile Strength Effect phenomenon [26].

Figure 7 summarizes the results of the thermogravimetric (TG) measurements. These data (also listed in Table 1) allow the analyses of the thermochemical reaction (Eq. 1) and interactions between Cg and $SrBr_2$. The TG measurement data shown in Fig. 7 clearly indicate that the dehydration reaction occurs in two distinct steps with one step losing five H_2O molecules and the other step losing one H_2O molecule, in line with previous investigations on pure $SrBr_2$ [22,27] The onset temperatures of the two reaction steps are respectively at 64.7°C and 160.1°C. The total water loss of the TCS composite in the two steps is in line with theoretical predictions: the composites with 40% and 80% $SrBr_2$ give respectively 40% and 80% water loss expected by pure $SrBr_2 \cdot 6H_2O$. Interestingly, Figure 7 shows the presence of Cg matrix leads to a reduction in the onset temperature evidenced by the shift of the thermogravimetric curve towards a lower temperature. This shift is

significant with the onset temperature of the first reaction step (48.2°C) decreasing by ~16°C for the TCS composite with 40% of $SrBr_2$.

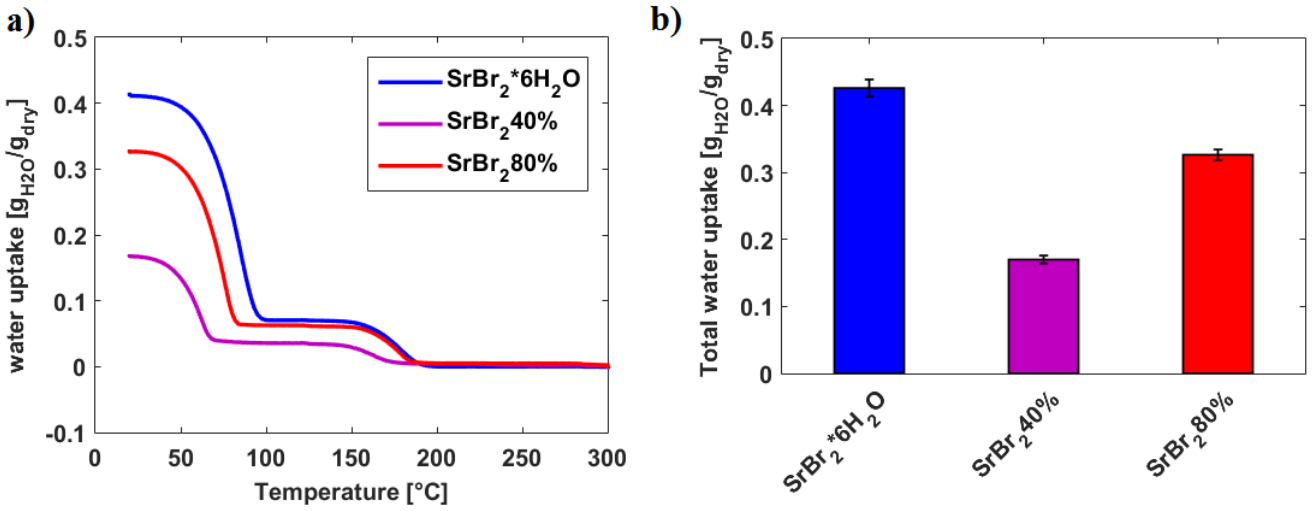

Fig. 7. Thermogravimetric analysis (TG) of pure $SrBr_2$ and TCS composites showing two dehydration steps with the onset temperatures depending of the graphite contents, and the overall mass change in line with theoretical predictions.

The results of the differential scanning calorimetry (DSC) analyses are demonstrated in Figure 8. One can see clearly that the thermochemical reaction occurs in two distinct steps for all TCS composites, and the onset temperature shifts toward a lower temperature. These results are in agreement with the TG measurements discussed above. The DSC curves also show that peak height and the area under the peak decrease with increasing amount of Cg addition in the TCS composites as the matrix does not participate in the reaction (although Cg may contribute to the kinetics due to its effect on heat and mass transfer). The integration of DSC curves gives the heat of reaction, which are presented in Figure 8b and also Table 1. The experimentally measured heat of reaction of the TCS composites is in line with the theoretical prediction obtained by simply weight averaging the heat of reaction of pure $SrBr_2{\cdot}6H_2O$ salt. This suggests that the interactions between the Cg matrix and $SrBr_2$ affect primarily the kinetic of the reaction (e.g. the onset temperature) rather than heat of reaction.

Furthermore, DSC and TG results shows that the traces impurities in the graphite (0.05% Sulphur, 0.05% Nitrogen, 0.8% ash, 0.3% Volatile, 0.3% Moisture) do not affect the performance of the TCS composite. No mass-change steps of endothermic/exothermic were found beside those associated to hydration/dehydration of SrBr2, confirming that impurities in the graphite are negligible and no relevant side reactions occurs.

The DSC analyses also give the specific heat of the TCS composites by using the ISO 11357–4 procedure [28]. Figure 9a shows the results over the temperature range of interest in this work; see also Table 1. By using the specific heat capacity data and the reaction heat, one can obtain the energy density, e_t, by using the following equation:

$$e_t(T) = \underbrace{\int_{T_0}^{T} c_p(T)\,dT}_{sensible} + \underbrace{\int_{T_0}^{T} \frac{d}{dT}\Delta H(T)\,dT}_{thermochemical} \qquad (2)$$

The use of Equation 2 requires integration across the temperature range considered, which was done numerically with a second order quadrature scheme. For doing so, the experimentally measured specific heat was first curved fitted using a shape preserving spline interpolation method and the thermochemical contribution was directly

obtained from the differential scanning calorimetry data shown in Figure 8. One can see immediately the exceptional benefits of the TCS composites: considering a charging temperature of 80°C, as for example proposed in [19], the energy density can reach ~500kJ/kg and this same total energy density of the pure $SrBr_2$ can also be achieved by the TCS composites. It is relevant to emphasize that the energy density achieved by our hybrid composite is significant for the narrow temperature range considered (80°C charging); other composites proposed in the literature have achieved similar storage capacity only with larger temperature ranges (100°C or above) [12,29] Such advantage of our composite has the potential to significantly impact on the economics of the TCS systems – one can achieve the same with less than half of the hydrate and hence significant cost reduction – one of the key barriers preventing industrial uptake of the TCS technology [11]. If a temperature of 150ºC is considered, the energy density of the composites can exceed ~600kJ/kg. Although the pure salt at this temperature shows a higher energy density, this cannot fully used as will be discussed later in the paper. In addition, as shown in Figure 8 and Table 1, the sensible heat takes a significant portion of the total energy density, which clearly cannot be ignored as many publications on TCS.

Figure 10 shows the thermal conductivity of the TCS composites. The thermal conductivity of the composite with 40% of $SrBr_2$ is approximately five-fold higher than the pure SrBr2 and other pure salt hydrates [30,31] considered in the literature as potential candidate for thermochemical energy storage. Similarly, our TCS material shows higher thermal conductivity than composites using alluminosilicate minerals, for example zeolites, as support matrix [17]. This is clearly due to the exceptional heat transfer properties of the graphite. Such exceptional performance of the TCS composites help resolve another key issue of . energy storage materials – limited heat transfer performance [32,33]. At a TCS device level, heat transfer enhancement techniques are often used, e.g. fins, metallic meshes, to overcome the low thermal conductivity of pure salts [19,23,34], which increase the total cost of TCS devices due to the use of extra parts and more complex manufacture processes, and decreases the effective thermal energy storage density due to extra volume occupied by extra components. This demonstrates clear benefits in resolving the low thermal conductivity issue through the use of TCS composite materials.

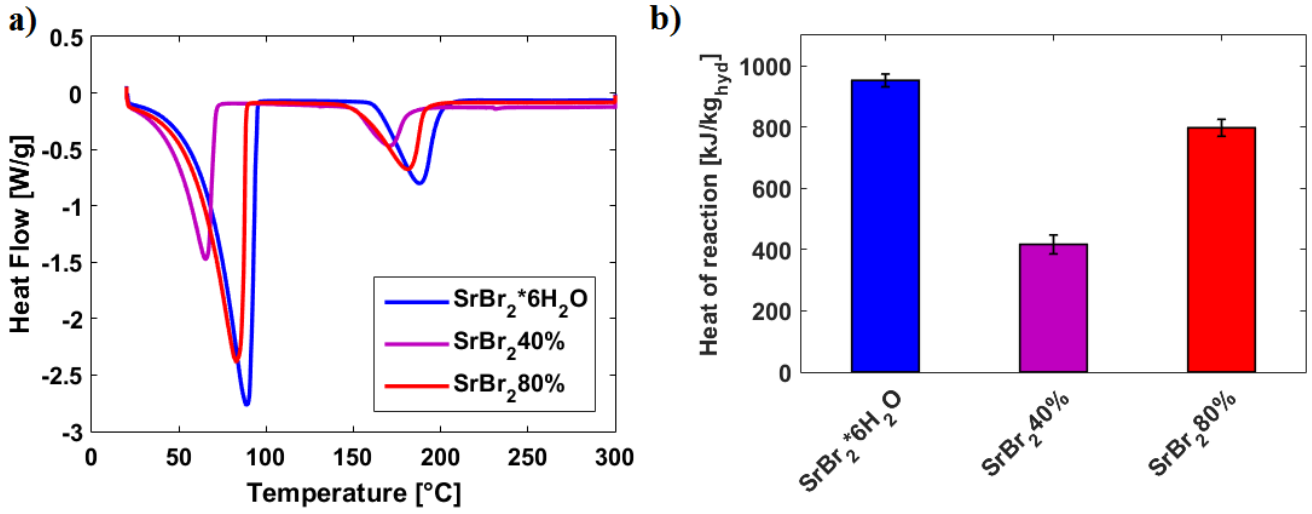

Fig. 8. Differential scanning calorimetry analysis of the pure $SrBr_2$ and the TCS composites: the heat of reaction decreases proportionally with the content of $SrBr_2$ in the composite; the presence of graphite decreases the onset temperature of the reaction.

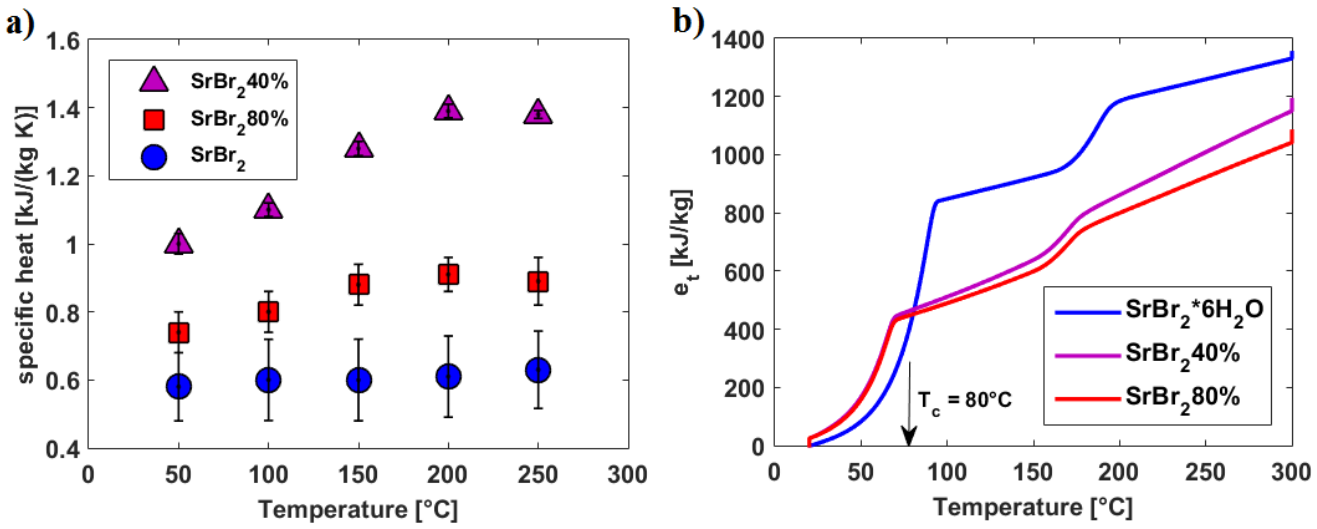

Fig. 9. Specific heat of pure $SrBr_2$ and the TCS composites: the TCS composites can store more sensible form of thermal energy due to increased in specific heat as a result of the addition carbon graphite.

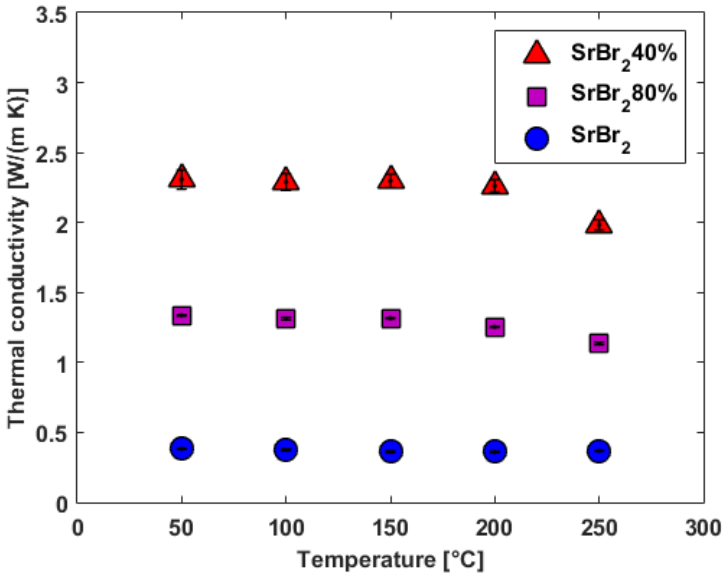

Fig. 10. Thermal conductivity of pure $SrBr_2$ and the TCS composites: thermal conductivity of the pure salt in line with that reported in [30]; a five-fold increase in thermal conductivity achieved by using TCS composites.

The results of the dynamic vapor sorption (DVS) analyses are summarized in Figure 11 with the hydration process was carried out at 25°C at a relative humidity of 50%. One can see a clear hysteresis of the charge-discharge cycle of the pure $SrBr_2$ with a residual water content of 5% at the end of the discharge process, indicating that the salt does not dehydrate completely even under RH=0%. This is likely attributable to the formation of a crust of dehydrated salt around the salt particle, which presents a very high mass transfer resistance to the dehydration of the core [12]. This has a detrimental effect on the actual thermal energy storage density as part of the stored energy is not actually accessible. The use of carbon graphite matrix in the TCS composites greatly reduces the hysteresis, indicating an improved mass transfer which contribute to overcome the cyclability issue of salts [35] We ascribe this to the channeling effect of the platy particles of carbon graphite as schematically illustrated in Figure 12. The carbon graphite supports the salt particles while at the same time provides transport channels for water molecules to reach the salt (hydration process during charge). Also, the

graphite particles also creates a highly conductive "thermal network", leading to an enhanced heat transfer as presented in Figure 10.

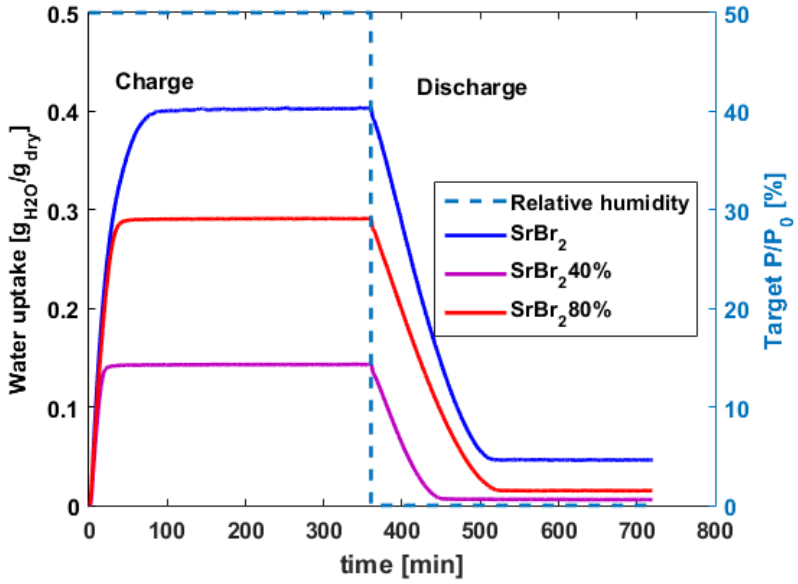

Fig. 11. Dynamic water sorption analysis at 25°C and 50% relative humidity: carbon graphite in the composite reduces the hysteresis, leading to nearly complete dehydration of the TCS composites.

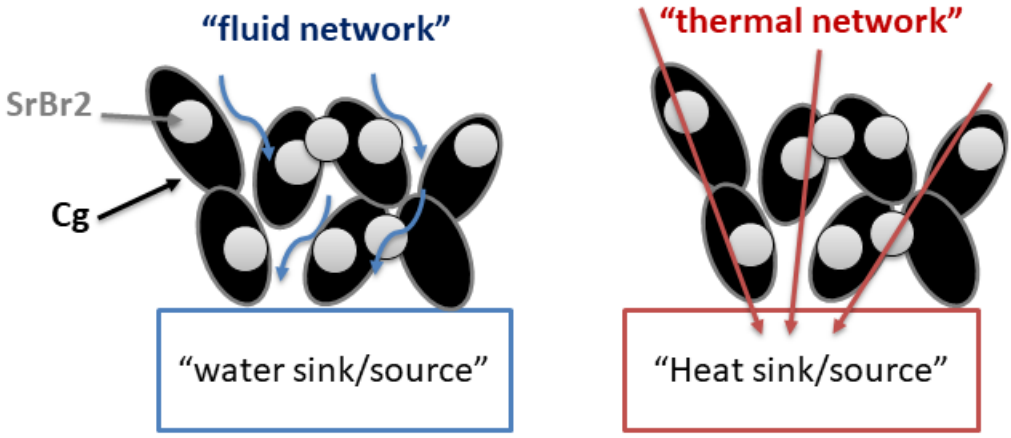

Fig. 12. Schematic diagram illustrating the enhancement mechanism of mass and heat transfer within the TCS composites.

Concluding remarks

We have formulated, characterized and successfully manufactured high performance thermochemical storage (TCS) composites consisting strontium bromide ($SrBr_2$) and carbon graphite and the following conclusions have been obtained:

- The $SrBr_2$ based TCS composites are suitable for thermal energy storage over a temperature range of 50-150°C. An energy storage density of 500kJ/kg can be achieved at a temperature of 80°C, and the energy density increases to ~600kJ/kg if the operating temperature is increased to 150°C. The TCS composites has a similar energy density to the pure $SrBr_2$ at a temperature up to ~80°C. The energy density of the

pure salt is higher than the TCS composite at temperatures higher than ~80°C, however, not all the energy stored can be discharged likely due to heat and mass transfer limitations.

- The use of carbon graphite in the composite formulation significantly increases the specific heat (up to four times compared to pure $SrBr_2$), implying a far high contribution of the sensible heat to the total energy density of the TCS composites.
- The use of graphite dramatically enhances the thermal conductivity of the TCS composites with a five-fold increase measured in this work.
- The use of carbon graphite improves not only the hydration/dehydration kinetics, shifting the onset of the reaction towards a lower temperature, but also reduces the hysteresis of hydration/dehydration cycle of the pure $SrBr_2$ salt, making deep charge-discharge possible.

In summary, we have shown how the formulation affects the TCS composite structure and hence their properties. This is for the first time for this promising materials system. More work is clearly needed to understand the underlying physics such as the exact reasons for the onset temperature shifting.

Acknowledgments

Dr A Sciacovelli and Prof Y Ding acknowledge the finance support from Engineering and Physical Sciences Research (EPSRC) Council, UK – SUPERGEN Energy Storage Hub (1EP/L019469/1), Energy Storage for Low Carbon Grids (EP/K002252/1), and NexGen-TEST Next Generation Grid Scale Thermal Energy Storage Technologies (EP/L014211/1). Dr A Dr Sciacovelli would like to thank Prof Paul Webley (University of Melbourne) for his useful suggestions on adsorption processes.

References

[1] Shifrin C. The heat is on. Nat Energy 2016;22:28–9. doi:10.1038/nphys2638.

[2] DECC. The Future of Heating: A strategic framework for low carbon heat in the UK. Dep Energy Clim Chang 2012:1–120.

[3] Teverson CLR. Doing cold smarter. 2015.

[4] Cot-gores J, Castell A, Cabeza LF. Thermochemical energy storage and conversion : A-state-of-the-art review of the experimental research under practical conditions. Renew Sustain Energy Rev 2012;16:5207–24. doi:10.1016/j.rser.2012.04.007.

[5] Cabeza LF, Solé A, Barreneche C. Review on sorption materials and technologies for heat pumps and thermal energy storage. Renew Energy 2016. doi:10.1016/j.renene.2016.09.059.

[6] Zhang H, Baeyens J, Cáceres G, Degrève J, Lv Y. Thermal energy storage: Recent developments and practical aspects. Prog Energy Combust Sci 2016;53:1–40. doi:10.1016/j.pecs.2015.10.003.

[7] Solé A, Martorell I, Cabeza LF. State of the art on gas – solid thermochemical energy storage systems and reactors for building applications. Renew Sustain Energy Rev 2015;47:386–98. doi:10.1016/j.rser.2015.03.077.

[8] Michel B, Mazet N, Neveu P. Experimental investigation of an innovative thermochemical process operating with a hydrate salt and moist air for thermal storage of solar energy : Global performance. Appl Energy 2014;129:177–86. doi:10.1016/j.apenergy.2014.04.073.

[9] Scapino L, Zondag HA, Van Bael J, Diriken J, Rindt CCM. Sorption heat storage for long-term low-temperature applications: A review on the advancements at material and prototype scale. Appl Energy 2017;190:920–48. doi:10.1016/j.apenergy.2016.12.148.

[10] Henninger SK, Ernst SJ, Gordeeva L, Bendix P, Frohlich D, Grekova AD, et al. New materials for adsorption heat transformation and storage. Renew Energy 2016. doi:10.1016/j.renene.2016.08.041.

[11] Scapino L, Zondag HA, Van Bael J, Diriken J, Rindt CCM. Energy density and storage capacity cost comparison of conceptual solid and liquid sorption seasonal heat storage systems for low-temperature space heating. Renew Sustain Energy Rev 2017;76:1314–31. doi:10.1016/j.rser.2017.03.101.

[12] Casey SP, Elvins J, Riffat S, Robinson A. Salt impregnated desiccant matrices for "open" thermochemical energy storage - Selection, synthesis and characterisation of candidate materials. Energy Build 2014;84:412–25. doi:10.1016/j.enbuild.2014.08.028.

[13] N'Tsoukpoe KE, Schmidt T, Rammelberg HU, Watts BA, Ruck WKL. A systematic multi-step screening of numerous salt hydrates for low temperature thermochemical energy storage. Appl Energy 2014;124:1–16. doi:10.1016/j.apenergy.2014.02.053.

[14] Rammelberg HU, Osterland T, Priehs B, Opel O, Ruck WKL. Thermochemical heat storage materials - Performance of mixed salt hydrates. Sol Energy 2016;136:571–89. doi:10.1016/j.solener.2016.07.016.

[15] N'Tsoukpoe KE, Osterland T, Opel O, Ruck WKL. Cascade thermochemical storage with internal condensation heat recovery for better energy and exergy efficiencies. Appl Energy 2016;181:562–74. doi:10.1016/j.apenergy.2016.08.089.

[16] Fopah-Lele A, Tamba JG. A review on the use of SrBr2·6H2O as a potential material for low temperature energy storage systems and building applications. Sol Energy Mater Sol Cells 2017;164:175–87. doi:10.1016/j.solmat.2017.02.018.

[17] Tanashev YY, Krainov A V., Aristov YI. Thermal conductivity of composite sorbents "salt in porous matrix" for heat storage and transformation. Appl Therm Eng 2013;61:401–7. doi:10.1016/j.applthermaleng.2013.08.022.

[18] Shkatulov A, Aristov Y. Modi fi cation of magnesium and calcium hydroxides with salts : An ef fi cient way to advanced materials for storage of middle-temperature heat. Energy 2015;85:667–76. doi:10.1016/j.energy.2015.04.004.

[19] Zhao YJ, Wang RZ, Zhang YN, Yu N. Development of SrBr 2 composite sorbents for a sorption thermal energy storage system to store low-temperature heat 2016;115. doi:10.1016/j.energy.2016.09.013.

[20] Courbon E, Ans PD, Permyakova A, Skrylnyk O, Steunou N, Degrez M, et al. A new composite sorbent based on SrBr 2 and silica gel for solar energy storage application with high energy storage density and stability. Appl Energy 2017;190:1184–94. doi:10.1016/j.apenergy.2017.01.041.

[21] Zhang YN, Wang RZ, Zhao YJ, Li TX, Riffat SB, Wajid NM. Development and thermochemical characterizations of vermiculite/SrBr2 composite sorbents for low-temperature heat storage. Energy 2016;115:120–8. doi:10.1016/j.energy.2016.08.108.

[22] Michel B, Mazet N, Neveu P. Experimental investigation of an open thermochemical process operating with a hydrate salt for thermal storage of solar energy : Local reactive bed evolution. Appl Energy 2016;180:234–44. doi:10.1016/j.apenergy.2016.07.108.

[23] Fopah A, Kuznik F, Opel O, Ruck WKL. Performance analysis of a thermochemical based heat storage as an addition to cogeneration systems. Energy Convers Manag 2015;106:1327–44. doi:10.1016/j.enconman.2015.10.068.

[24] Goldstein J, Newbury DE, Joy DC, Lyman CE, Echlin P, Lifshin E, et al. Scanning Electron Microscopy and X-ray Microanalysis. 3rd ed. New York: Springer Berlin Heidelberg; 2003.

[25] Rouquerol F, Rouquerol I, Sing K. Adsorption by Powders and Porous Solids - Principles, Methodology and Applications. London: Academic Press; 2013.

[26] Groen JC, Peffer LAA, Javier P. Pore size determination in modified micro- and mesoporous materials . Pitfalls and limitations in gas adsorption data analysis. Microporous Mesoporous Mater 2003;60:1–17. doi:10.1016/S1387-1811(03)00339-1.

[27] Richter M, Habermann E-M, Siebecke E, Linder M. A systematic screening of salt hydrates as materials for a thermochemical heat transformer. Thermochim Acta 2017;659:136–50. doi:10.1016/j.tca.2017.06.011.

[28] ISO IS. 11357-4, Determination of specific heat capacity 2005;2005.

[29] Jabbari-Hichri A, Bennici S, Auroux A. Enhancing the heat storage density of silica–alumina by addition of hygroscopic salts (CaCl2, Ba(OH)2, and LiNO3). Sol Energy Mater Sol Cells 2015;140:351–60. doi:10.1016/j.solmat.2015.04.032.

[30] Fopah Lele A, Edem N 'tsoukpoe K, Osterland T, Ed Eric Kuznik F, Ruck WKL. Thermal conductivity measurement of thermochemical storage materials. Appl Therm Eng 2015;89:916–26. doi:10.1016/j.applthermaleng.2015.06.077.

[31] Kleiner F, Posern K, Osburg A. Thermal conductivity of selected salt hydrates for thermochemical solar heat storage applications measured by the light flash method. Appl Therm Eng 2017;113:1189–93. doi:10.1016/j.applthermaleng.2016.11.125.

[32] N'Tsoukpoe KE, Restuccia G, Schmidt T, Py X. The size of sorbents in low pressure sorption or thermochemical energy storage processes. Energy 2014;77:983–98. doi:10.1016/j.energy.2014.10.013.

[33] Gaeini M, Zondag HA, Rindt CCM. Effect of kinetics on the thermal performance of a sorption heat storage reactor. Appl Therm Eng 2016;102:520–31. doi:10.1016/j.applthermaleng.2016.03.055.

[34] Fopah-lele A, Rohde C, Neumann K, Tietjen T, Ruck WKL. Lab-scale experiment of a closed thermochemical heat storage system including honeycomb heat exchanger. Energy 2016;114:225–38. doi:10.1016/j.energy.2016.08.009.

[35] Donkers PAJ, Pel L, Adan OCG. Experimental studies for the cyclability of salt hydrates for thermochemical heat storage. J Energy Storage 2016;5:25–32. doi:10.1016/j.est.2015.11.005.